Ultrastructural Investigation of Resistant and Susceptible Maize Inbreds Infected with *Erwinia stewartii*

E. J. Braun

Assistant professor, Department of Plant Pathology, Seed and Weed Sciences, Iowa State University, Ames 50011.Project No. 2194 and Journal Paper J-10021 of the Iowa Agriculture and Home Economics Experiment Station, Ames.
Supported by a grant from the Iowa State University Research Foundation.
Electron microscopy was done in the Bessey Hall Microscopy Facility, Department of Botany, Iowa State University.
Accepted for publication 11 March 1981.

ABSTRACT

Braun, E. J. 1982. Ultrastructural investigation of resistant and susceptible maize inbreds infected with *Erwinia stewartii*. Phytopathology 72:159-166.

Anatomical changes associated with the development of Stewart's wilt were studied in resistant (C123) and susceptible (B14A) maize inbred lines by using light and transmission electron microscopy. Pathogen populations increased at similar rates in leaves of resistant and susceptible plants. When leaves of maize plants at the tasseling stage were inoculated with *Erwinia stewartii*, lesions expanded three to four times more rapidly in B14A than in C123. In both lines, microscopic examination of lesions showed that pit membranes became coated with material resembling bacterial exopolysaccharide (EPS) while pathogen populations in vessels remained very low. As populations increased in vessels, many became occluded totally with bacterial cells and EPS. Four other types of material, assumed to be of host origin, also were found in vessels of infected plants. These materials, which could be differentiated on the basis of ultrastructural appearance and histochemical staining reactions, were found more frequently in C123 than in B14A, and they might possibly function in the localization of the pathogen.

Stewart's bacterial wilt and leaf blight, caused by *Erwinia stewartii* (E. F. Smith) Dye, is a serious disease of maize (*Zea mays* L.) in North America. Young, susceptible plants that become systemically infected with the bacterium can either wilt and die as seedlings or remain stunted. The leaf blight phase of the disease, which is of primary importance on dent maize, occurs after anthesis. Elongated lesions that develop on leaves commonly originate at feeding scars produced by corn flea beetles (*Chaetocnema pulicaria* Melsh.), the most important vector of the Stewart's wilt pathogen. Leaf lesions on resistant plants are smaller and less numerous than those on susceptible plants (15).

This cytological study was undertaken to gain information concerning the nature of resistance to the leaf blight phase of the disease. Particular attention was paid to the role of bacterial exopolysaccharide in disease development because this material is thought to be an important factor contributing to pathogen aggressiveness (15,22). Previous histological studies of the Stewart's wilt disease were concerned with the early season wilt phase of the disease (11,22).

MATERIALS AND METHODS

Plant and pathogen material. Yellow dent maize inbred lines C123 (resistant) and B14A (susceptible) were used throughout this investigation. The pathogen strain used in this study was a field isolate from Ohio that caused symptoms typical of Stewart's wilt in inoculated seedlings and adult plants. The pathogen was characterized as a strain of *E. stewartii* according to the criteria of Dye (3,4). The bacterium was a facultatively anaerobic, nonmotile, nonflagellate, Gram-negative rod that produced a yellow, water-insoluble pigment on nutrient agar. The bacterium failed to produce acetoin and it did not liquefy gelatin. Bacterial cultures were maintained on nutrient agar slants at 4 C. Pathogenicity of stock cultures was maintained by periodic inoculation and then reisolation from B14A seedlings. Preceding all experiments, stock cultures of the pathogen were inoculated into and reisolated twice from C123 seedlings to increase pathogen aggressiveness.

Pathogen growth in vivo. Twelve- to 14-day-old seedlings were inoculated by using a partial vacuum infiltration procedure to introduce bacteria into the intercellular spaces of the leaf. Seedling leaves were immersed in an aqueous bacterial suspension (10^7 cells per milliliter) containing 0.1% Triton X-100. A 0.518 kg/cm^2 vacuum was applied for 1 min and then released quickly. This process was repeated once. Seedlings were then rinsed in tap water.

Inoculated plants were placed in a growth chamber maintained at 27 C with a 14-hr photoperiod at 17,000 lux. Humidity was not monitored. Plants were fertilized once with a complete fertilizer (Miracle-Gro, Stearn's Nurseries, Inc., Geneva, NY 14456) just before inoculation.

At intervals of 0, 0.5, 1, 2, 3, 4, 5, and 7 days after inoculation, four leaf disks (0.48-cm diameter) were obtained from the third leaf of each of 10 plants. Leaf disks were washed in sterile distilled water, divided into four groups of 10 disks each, and ground in sterile phosphate buffer containing 0.1% Triton X-100. Samples were then serially diluted in sterile distilled water and plated on nutrient agar. Plates were incubated at 24 C, and colonies were counted after 4–5 days.

Lesion expansion. The eighth and ninth leaves of tasseling, greenhouse-grown, resistant and susceptible plants were inoculated by using a pinprick inoculation device (2) that had been dipped in an aqueous suspension of bacteria (10^7 cells per milliliter). Lesion areas were determined on five resistant and five susceptible plants at 1, 2, and 3 wk after inoculation.

Microscopy. Samples for both light and electron microscopy were fixed 6 hr at room temperature in 5% glutaraldehyde in 0.05M phosphate buffer, pH 6.8. Samples were then washed in buffer and postfixed overnight at 4 C in 1% OsO_4 in phosphate buffer. Tissue samples were then washed in buffer, dehydrated in ethanol, transferred to propylene oxide, and embedded in an Epon-Araldite mixture.

Thin sections for transmission electron microscopy (TEM) and adjacent thick sections for light microscopy (LM) were cut with glass knives. Thin sections were picked up on uncoated 74-μm (200-mesh) grids, stained with uranyl acetate and lead citrate, and examined with a Hitachi HU 11-C electron microscope. Thick sections were affixed to glass slides and stained with either toluidine blue O (a general metachromatic stain), Sudan black B (SB) for lipids and tannins (14), or Schiff's reagent for total insoluble carbohydrates (16). Specimens were viewed and photographed by using bright field optics.

Sampling of tissue for microscopy. B14A seedlings were inoculated by using a partial-vacuum infiltration procedure to study the appearance of *E. stewartii* as its populations developed in vivo. Inoculum consisted of bacterial cells harvested from nutrient agar

The publication costs of this article were defrayed in part by page charge payment. This article must therefore be hereby marked "*advertisement*" in accordance with 18 U.S.C. § 1734 solely to indicate this fact.

0031-949X/82/001015908/$03.00/0

slants and washed repeatedly by centrifugation in sterile distilled water. Leaf tissue samples were collected at 1, 3, 12, 30, and 96 hr after inoculation and processed for TEM.

Observations of host-parasite interactions during the leaf blight phase of the disease were made by using leaves of tasseling maize plants inoculated by the pinprick method. At 1, 2, and 3 wk after inoculation, samples were obtained from healthy and infected C123 and B14A plants and processed for LM and TEM. Sampling date and position with respect to inoculation wounds and lesion margin were recorded. At least two tissue blocks from each of three different plants were examined for each position and sampling date.

RESULTS

Lesion development and pathogen growth in vivo. Lesions became visible on leaves of tasseling maize plants about 1 wk after inoculation. Small, gray-green spots developed around each inoculation wound, and these spots coalesced as lesions expanded. Lesions expanded both acropetally and basipetally so that wounds always remained near the center of the lesions. Lesions expanded much more rapidly in B14A than in C123 (Fig. 1). Three weeks after inoculation, lesions were more than four times larger in the susceptible inbred. As lesions enlarged, infected tissues become flaccid and, eventually, necrotic.

Growth of the pathogen was examined in B14A and C123 seedlings. Pathogen populations increased similarly in both inbreds (Fig. 2). Although populations were somewhat greater in B14A, differences generally were not significant.

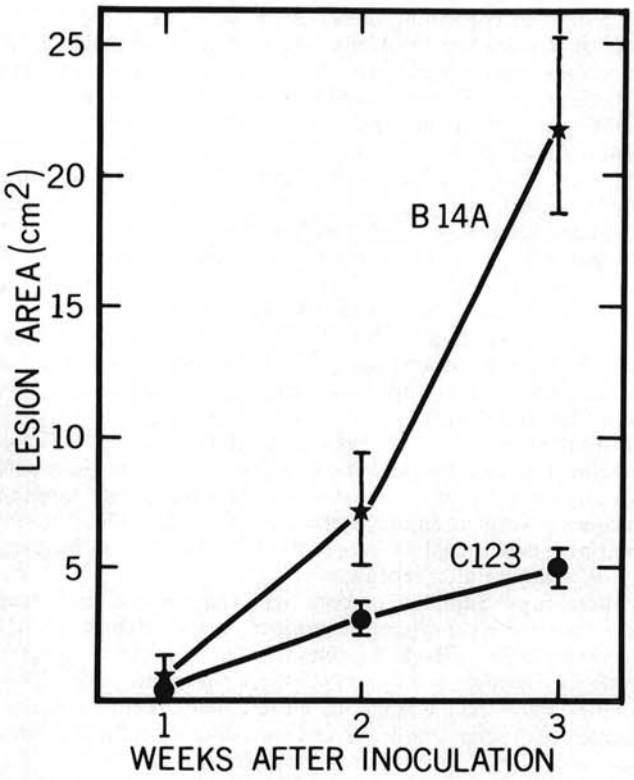

Fig. 1. Lesion areas on leaves of maize inbred lines B14A (susceptible) and C123 (resistant) inoculated at the tasseling stage with *Erwinia stewartii*. Bars indicate standard errors.

Anatomy of healthy maize leaves. The histology of healthy maize leaves (Fig. 3) is discussed elsewhere (5). For future reference, the ultrastructural appearance of vascular parenchyma cells and pit membranes are described in some detail. Vascular parenchyma cells in mature maize leaves were highly vacuolate (Fig. 4). In addition, nuclei, plastids, and mitochondria were present. A moderate amount of endoplasmic reticulum (ER) was observed in most cells, whereas dictyosomes were generally few in number.

Metaxylem vessels had cell walls with scalariform-to-reticulate, pitted secondary thickenings. Pit pairs between adjacent vessels contained wall material consisting of a loose meshwork of fibrils (Fig. 5). This wall material, which is referred to as a pit membrane, is formed when noncellulosic components are removed from primary wall material during the final stages of vessel element maturation (6).

Observations of developing pathogen populations. At 1 and 3 hr after vacuum infiltration of B14A seedlings, bacteria were found singly or in small groups in intercellular spaces. A small amount of fibrillar material could be seen outside bacterial cell walls (Fig. 6). At 12 hr after inoculation, a well-developed capsule, composed of material thought to be bacterial exopolysaccharide (EPS), was seen surrounding *E. stewartii* cells (Fig. 7). Some EPS appeared to be sloughing off bacterial cells into the surrounding medium. By 30 hr after inoculation, small colonies of bacteria were present. EPS was seen surrounding pathogen cells and accumulating on host cell walls close to bacterial colonies (Fig. 8). Four days after inoculation, *E. stewartii* populations were in the stationary phase of growth. Large colonies were scattered throughout the intercellular spaces of the inoculated leaves. Bacterial cells were embedded in dense accumulations of material believed to be EPS (Fig. 9). This material was Schiff-positive, stained reddish-purple with toluidine blue O, and had a granular appearance when observed with TEM. At this time, many bacterial cells appeared to be degenerating; cytoplasm was uniformly dense and cell shape was often irregular. In addition, small vesicles seemed to be forming around the periphery of some organisms (Fig. 9).

Observations of leaf blight infections in resistant and susceptible plants. Unless otherwise noted, all phenomena described were observed routinely in both B14A and C123. The pathogen initially

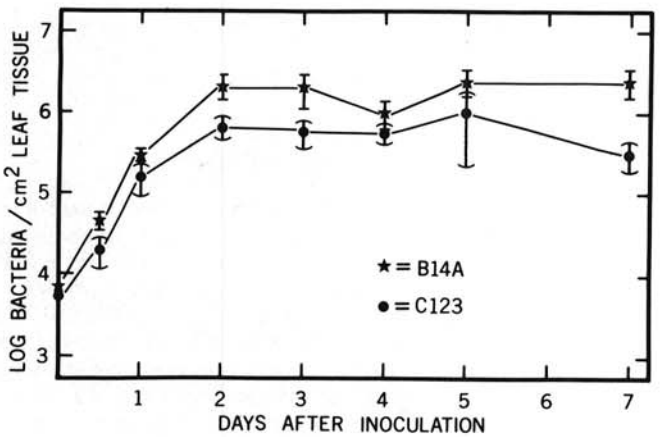

Fig. 2. Growth of *Erwinia stewartii* in resistant (C123) and susceptible (B14A) inbred maize seedlings. Bars indicate standard errors.

Figs. 3–9. 3, Cross section of healthy maize leaf (C123). Major vein (left) and minor vein (right) are delimited by bundle sheaths (bs). Phloem (ph), protoxylem lacuna (pl), wide metaxylem vessels (large arrowhead) and narrow metaxylem vessels (small arrowhead) can be seen within a major vein. Arrow denotes stomate. Bar represents 10 μm. **4,** Xylem parenchyma cell from major vein in a healthy maize plant (B14A). Wide metaxylem vessel is adjacent to parenchyma cell wall (cw). Parenchyma protoplast contains a nucleus (N), mitochondria (m), and large vacuoles (Va). Arrowheads denote endoplasmic reticulum. Bar represents 1 μm. **5,** Pit membrane (PM) and vessel cell walls (cw) between adjacent vessels in metaxylem of major vein in a healthy maize plant (C123). Bar represents 1 μm. **6,** *Erwinia stewartii* cells (B) in intercellular space 3 hr after infiltration into B14A maize seedling leaf. Bar represents 0.5 μm. **7,** Bacterial cells (B) near mesophyll cell (ME) in intercellular space 12 hr after infiltration into B14A maize seedling leaf. Pathogen cells are surrounded by a capsule of fibrillar exopolysaccharide (EPS). Bar represents 1 μm. **8,** *E. stewartii* cell (B) in intercellular space 30 hr after infiltration into B14A maize seedling leaf. Exopolysaccharide (EPS) surrounds bacterial cell and is on wall of adjacent mesophyll cell (ME). Bar represents 1 μm. **9,** Pathogen cells (B) within dense polysaccharide matrix (EPS) adjacent to mesophyll cell (ME) 4 days after infiltration into B14A maize seedling leaf. Bar represents 1 μm.

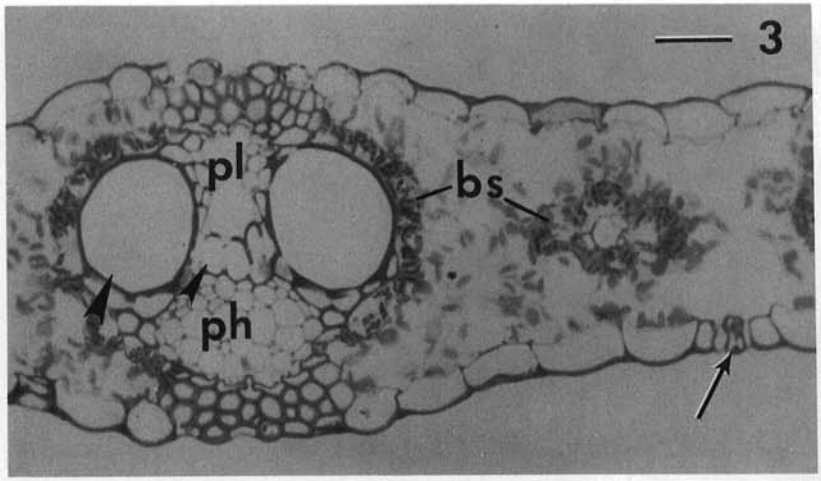
3
pl
bs
ph

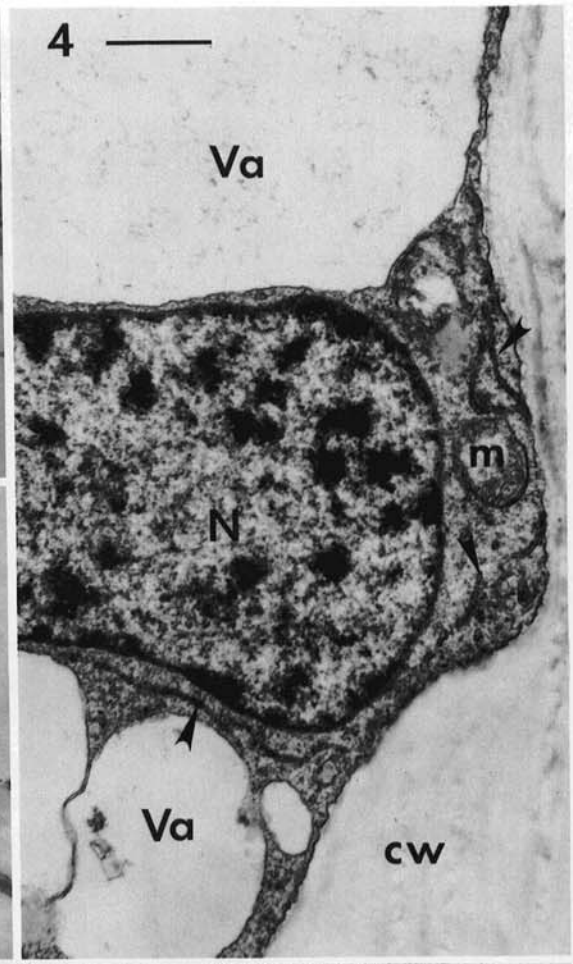
4
Va
m
N
Va
cw

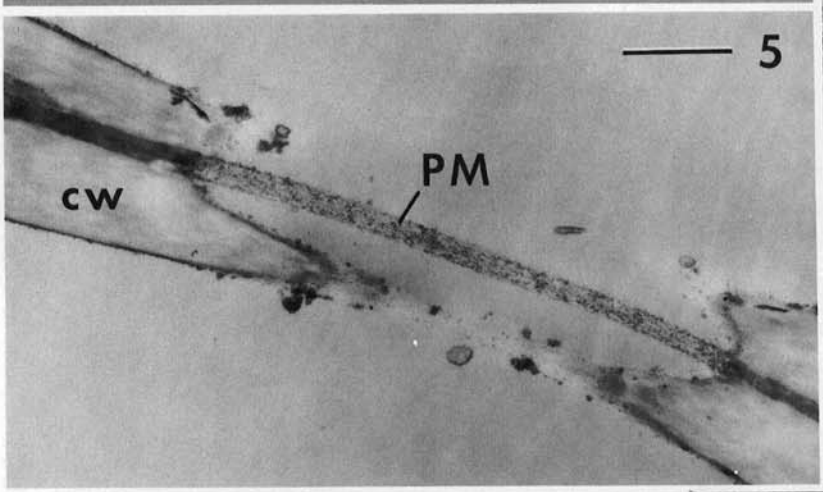
5
cw
PM

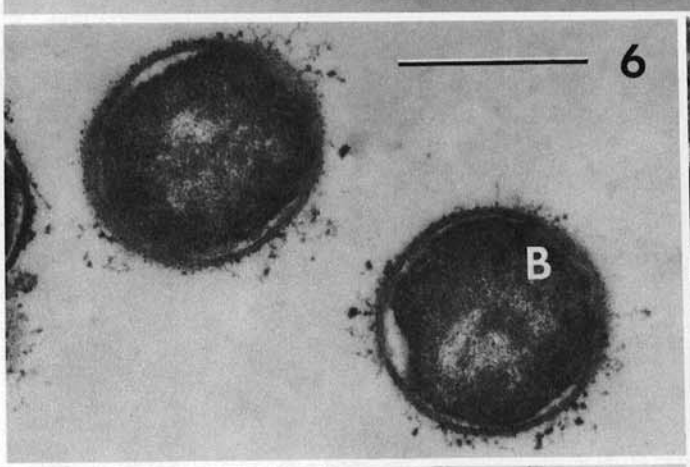
6
B

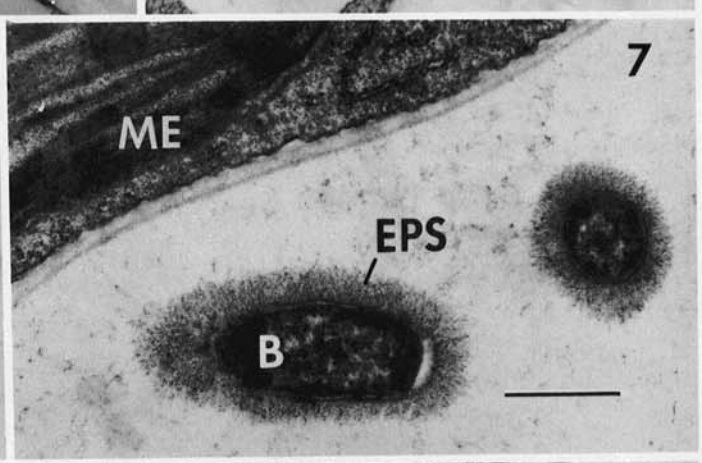
7
ME
EPS
B

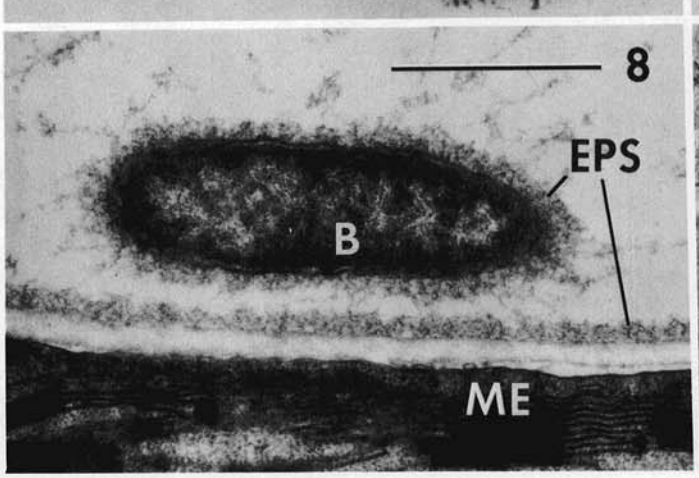
8
EPS
B
ME

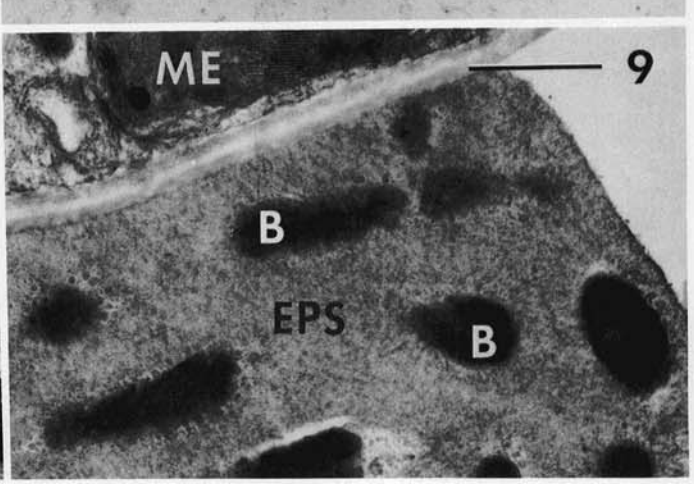
ME
9
B
EPS
B

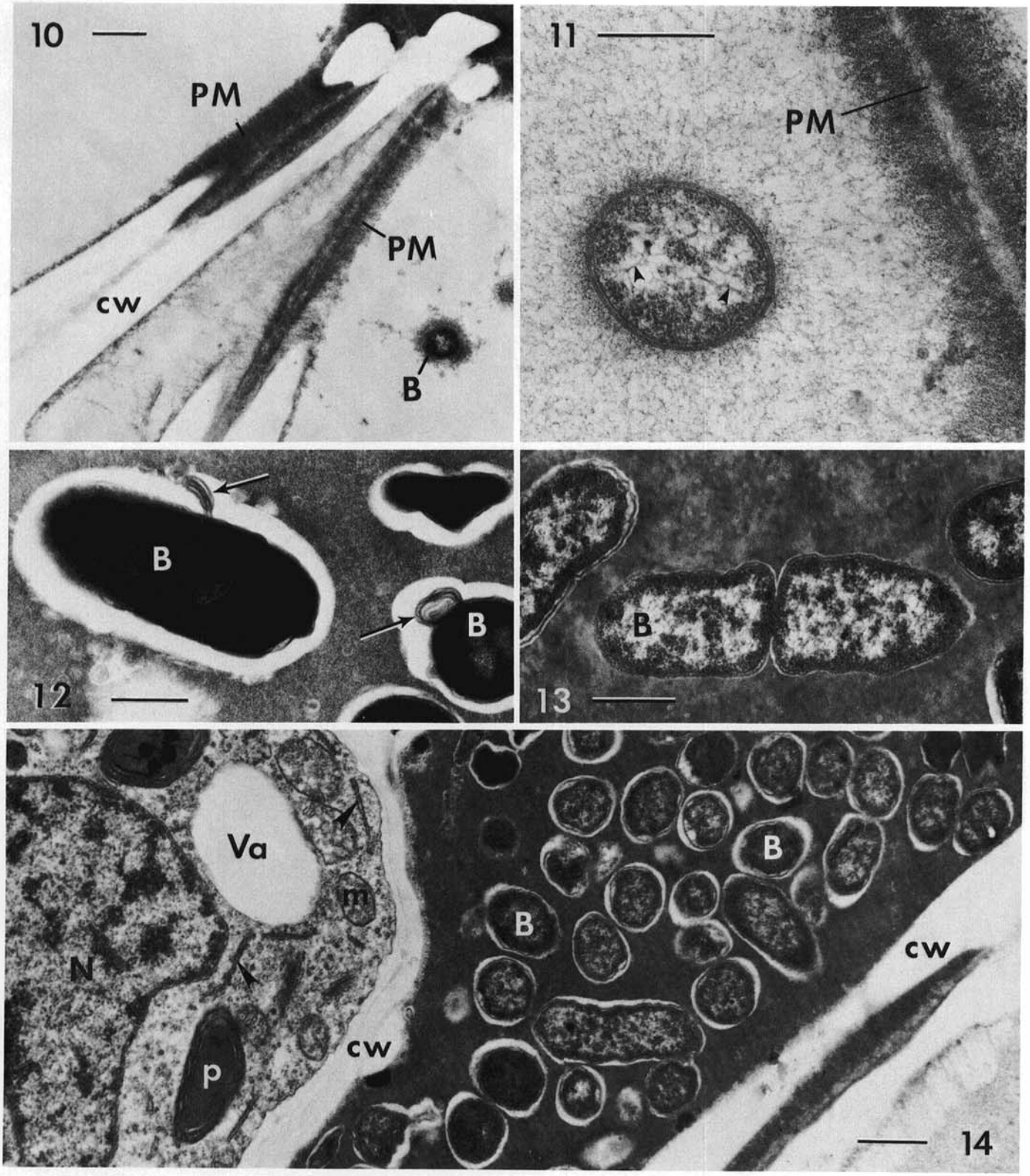

Figs. 10–14. *Erwinia stewartii* cells in xylem of infected maize leaves. **10,** *E. stewartii* cell (B) in lumen of narrow metaxylem vessel of tasseling C123 plant. Abundant EPS has accumulated on pit membranes (PM) while relatively little is in the vessel lumen or on vessel cell walls (cw). Sample was taken 1 cm outside lesion margin, 3 wk after inoculation. Bar represents 1 μm. **11,** Pathogen cell in minor vein vessel of B14A plant. Ribosome-rich region of bacterial cytoplasm surrounds nucleoid region containing fibrils of nucleic acid (arrowheads). EPS has accumulated on pit membrane (PM) and is distributed in vessel lumen as a loose network of fibrils. Sample was collected 1 cm outside lesion margin, 3 wk after inoculation. Bar represents 0.5 μm. **12,** Bacterial cells (B) embedded in EPS in narrow metaxylem vessel. Arrows denote vesiculation of outer membrane of bacterial cell wall. EPS matrix was Schiff-positive, stained reddish-purple with toluidine blue (TB), but did not stain with Sudan black B (SB). Sample was collected 1 wk after inoculation, 0.5 cm from inoculation wounds on C123 leaf. Bar represents 0.5 μm. **13,** Dividing *E. stewartii* cell (B) in EPS-occluded vessel of minor vein in C123 leaf. Sample taken at lesion margin 3 wk after inoculation. Bar represents 0.5 μm. **14,** Occluded vessel in minor vein of inbred B14A. Mass of bacterial cells (B) in EPS matrix is surrounded by vessel cell walls (cw). Adjacent mitochondria (m) and vacuoles (Va). Arrowheads denote endoplasmic reticulum. Bar represents 1 μm.

was confined to xylem vessels in infected leaves; eg, in samples collected 1 wk after inoculation, bacteria were observed only within xylem vessels. Vascular parenchyma cells (and occasionally phloem cells) were next to be invaded. *E. stewartii* cells were observed in intercellular spaces of the mesophyll only in the later stages of pathogenesis (inside lesion margins 2 and 3 wk after inoculation.)

Ultrastructurally, *E. stewartii* is a typical rod-shaped, Gram-negative bacterium. The bacterial cell wall consists of an outer membrane surrounding a thin peptidoglycan layer. The cell membrane is adjacent to the cell wall and the cytoplasm consists of an outer region containing abundant ribosomes and a central nucleoid with DNA fibrils (Fig. 11). A capsule of fibrillar EPS surrounds some bacteria (Fig. 10). In other instances, EPS

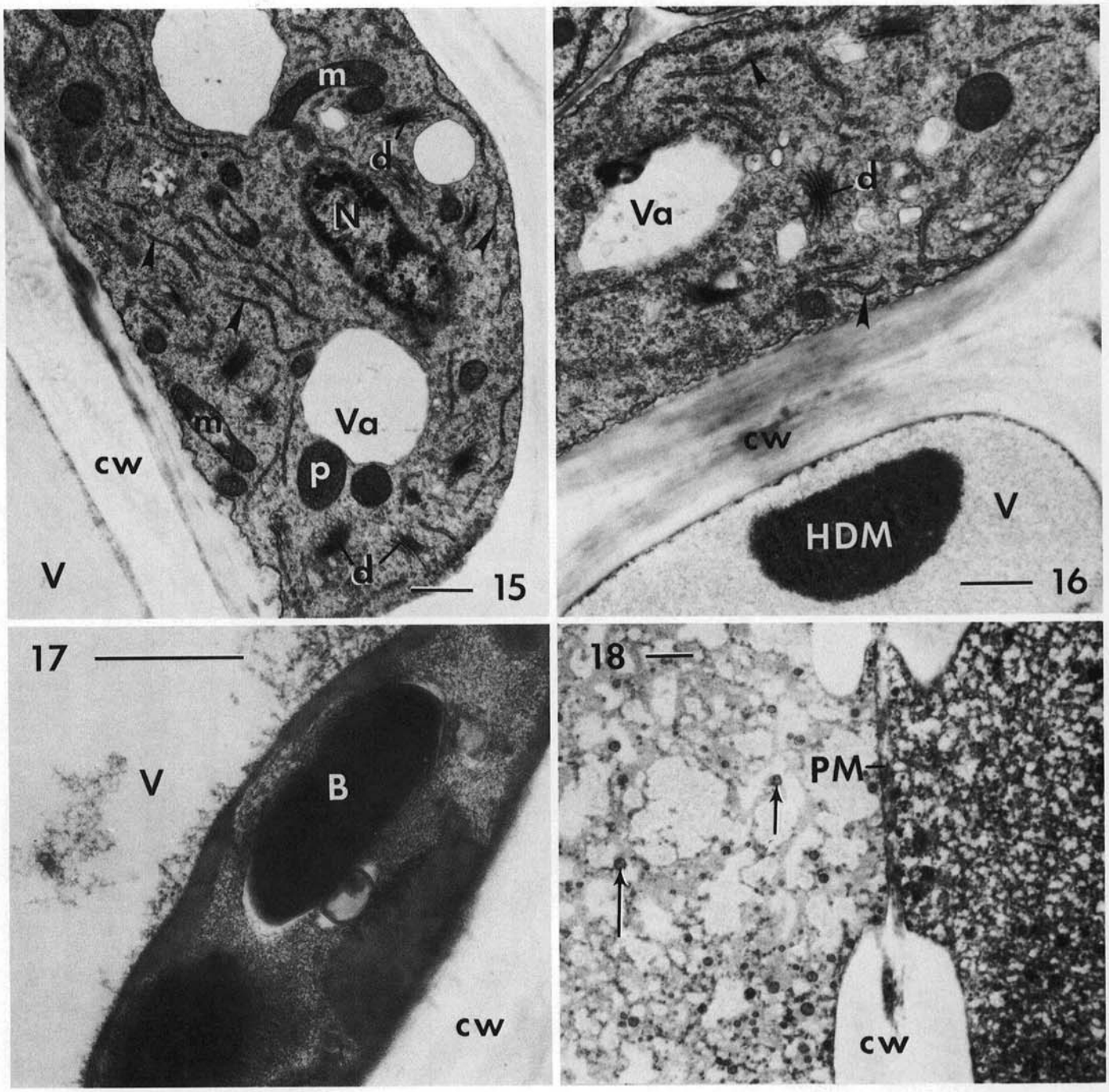

Figs. 15–18. Reactions of mature maize leaves infected with *Erwinia stewartii*. **15,** Metabolically active xylem parenchyma cell in sample collected 4 cm from inoculation wounds on a C123 leaf 1 wk after inoculation. Cell wall (cw) separates parenchyma cell from lumen of wide metaxylem vessel (V). A nucleus (N), mitochondria (m), plastids (p), dictyosomes (d), small vacuoles (Va), and abundant endoplasmic reticulum (arrowheads) can be seen within the parenchyma cell. Bar represents 1 μm. **16,** Metabolically active xylem parenchyma cell adjacent to narrow metaxylem vessel in major vein of C123 leaf. Host-derived material (HDM) can be seen within vessel lumen (V) and a small amount appears to have accumulated on the vessel cell wall (cw). HDM was Schiff-negative, Sudan black B (SB)-negative, and stained blue-purple with toluidine blue (TB). Small vacuoles (Va), dictyosomes (d), and abundant endoplasmic reticulum (arrowheads) can be seen within the parenchyma cell. Bar represents 1 μm. **17,** Bacterial cell (B) embedded in HDM in a wide metaxylem vessel. HDM has accumulated on the vessel cell wall (cw) and stained light purple with TB, was Schiff-positive and SB-negative. Some fibrous material can be seen within vessel lumen (V). Collected from C123 leaf 1 wk after inoculation, 0.5 cm from inoculation wounds. Bar represents 0.5 μm. **18,** Host-derived materials within narrow metaxylem vessels of major vein in C123 leaf. HDM stained dark blue with TB, was Schiff-positive, and was SB-positive. HDM contains diffuse material as well as small droplets (arrows). Vessel cell walls (cw) and pit membrane (PM) can be seen within accumulation of HDM. Sample collected outside lesion margin 3 wk after inoculation. Bar represents 1 μm.

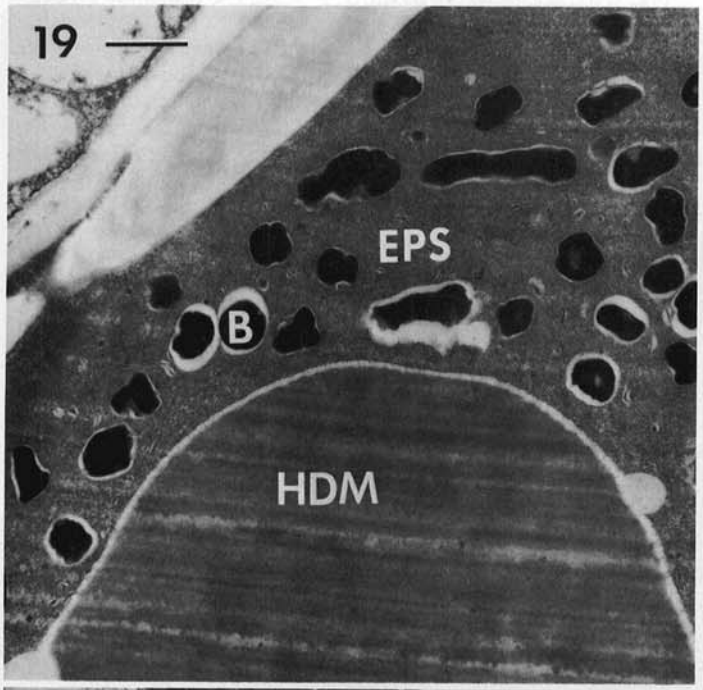
19
EPS
B
HDM

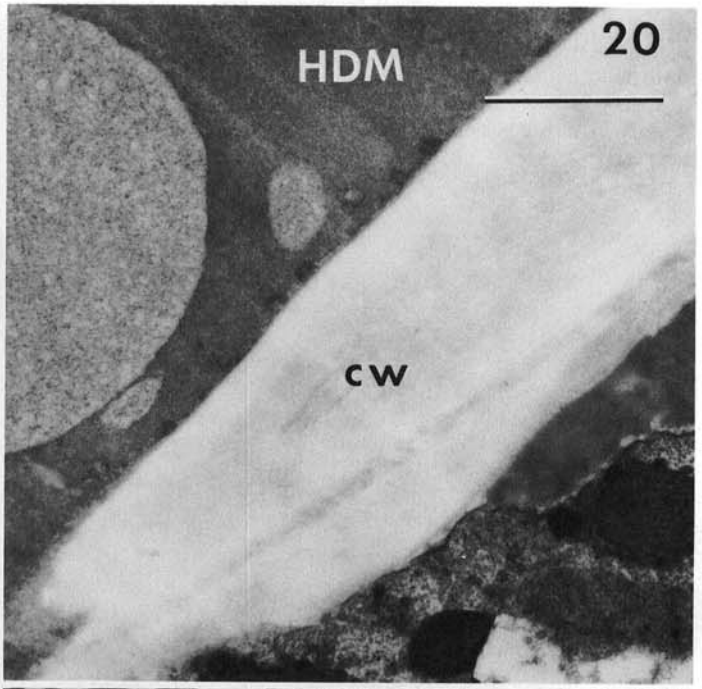
HDM
20
cw

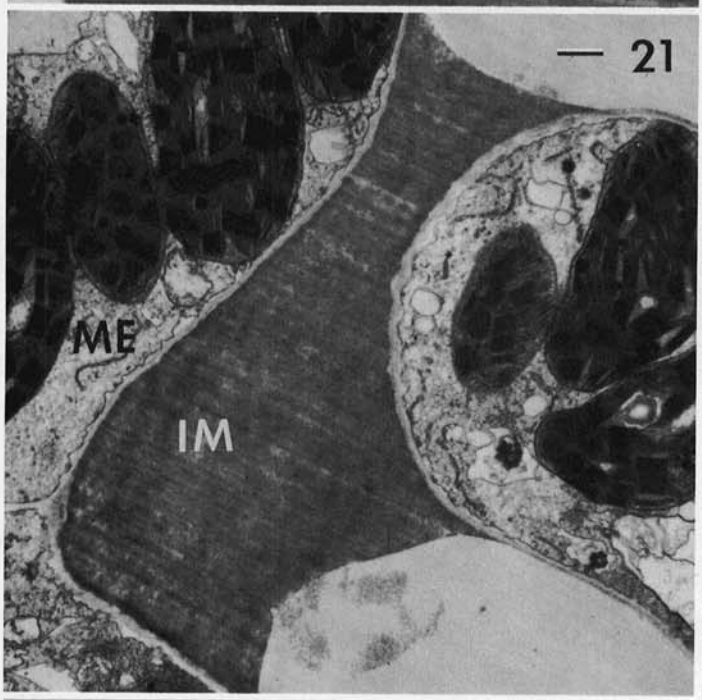
21
ME
IM

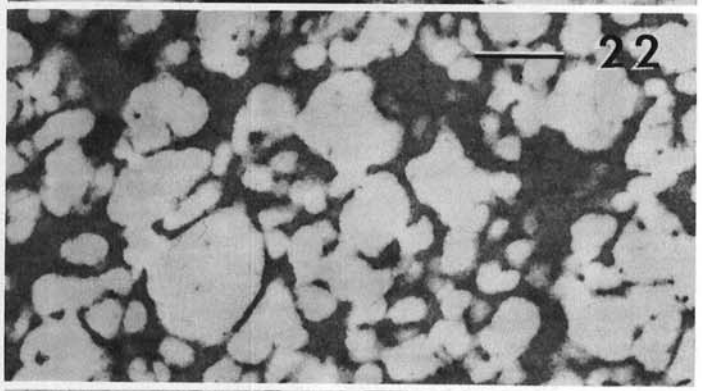
22

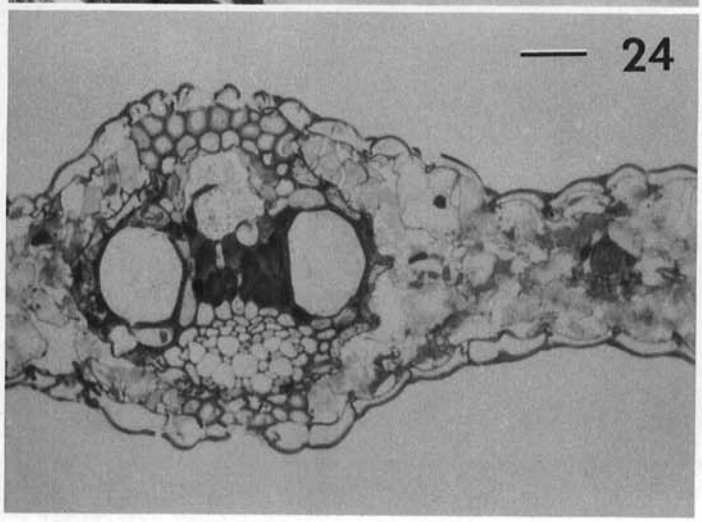
24

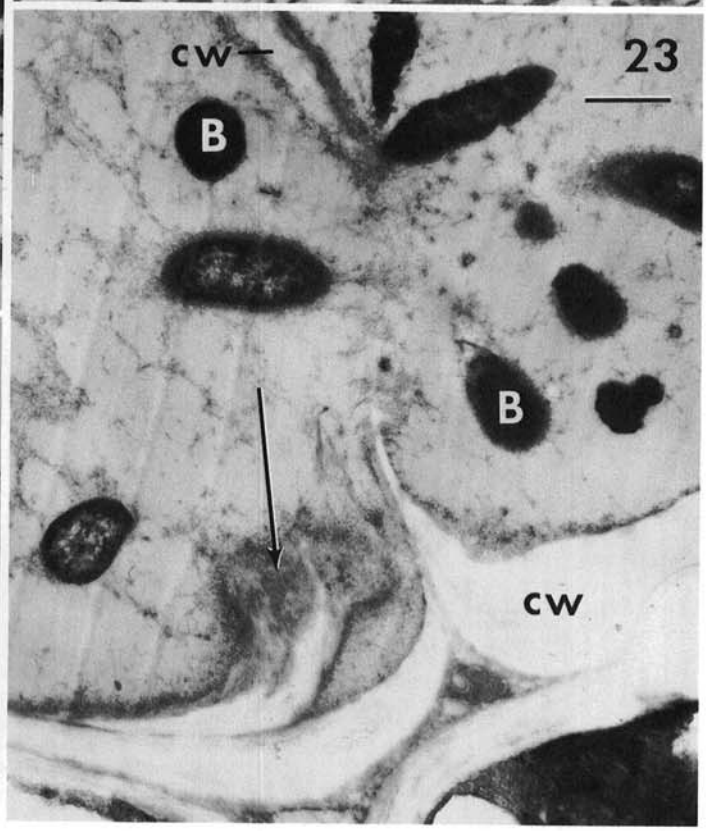
cw
23
B
B
cw

evidently is released into the vessel lumen where it forms a loose fibrillar network (Fig. 11).

In early stages of pathogenesis, material thought to be bacterial EPS was observed on vessel pit membranes (Figs. 10 and 11). Pit membranes often appeared completely coated with EPS, while pathogen populations within vessels were still very low. As pathogen populations increased, EPS accumulated within infected vessels until vessels supporting large populations usually were completely occluded with EPS (Figs. 12, 13, and 14). Accumulations of EPS were Schiff-positive, stained reddish-purple with toluidine blue O, and appeared granular when observed by TEM (Fig. 12). An electron-lucent area was commonly observed around bacterial cells embedded in dense accumulations of EPS (Figs. 12 and 14). This is possibly an artifact resulting from shrinkage of the highly hydrated EPS during preparation for microscopy.

Some pathogen populations in occluded vessels were composed primarily of cells thought to be senescent. Such cells were irregular in shape and had uniformly dense cytoplasm (Figs. 12 and 19). In addition, vesicles were associated with many of these cells. These vesicles, which probably arise from the outer wall membrane (Fig. 12), were frequently released and could be seen free within the EPS matrix. However, not all populations embedded in dense accumulations of EPS were moribund, and many populations in occluded vessels contained bacterial cells that appeared to be metabolically active (Fig. 13).

The earliest host response to infection was an apparent increase in the metabolic activity of xylem parenchyma cells (Figs. 15 and 16). These cells contained several small vacuoles and a dense cytoplasm in which numerous plastids and mitochondria were present. There also was a large increase in components of the endomembrane system (ER and dictyosomes). This apparent activity was elicited even in areas where pathogen cells were present in extremely low numbers.

At least four types of materials, assumed to be of host origin, were found in vessels of infected plants. These materials, which could be differentiated on the basis of their staining characteristics and ultrastructural appearance (see figure legends), were thought to be produced by host cells because they were often formed in areas where *E. stewartii* cells were rare or absent. It seems possible that metabolically active parenchyma cells were involved in deposition of these host-derived materials (HDM). Some types of HDM were found in both B14A and C123 (Figs. 16, 17, 18, and 19), whereas others were found only in C123 (Figs. 20 and 22). Some were found only in vessels in which *E. stewartii* cells were absent (Figs. 18, 20, and 22) whereas others occurred in vessels in the presence or absence of the pathogen (Figs. 16, 17, and 19).

Samples were collected from the area 2.5-5.0 mm outside the margins of 2-wk-old lesions to determine the frequency with which HDM were produced in B14A and C123. Ten lesions were sampled for each inbred. Sections were stained with toluidine blue O, observed with a light microscope, and the frequency of HDM-occluded vessels was recorded. In the minor veins, differences between B14A and C123 were not significant. Frequencies were 2.9 and 3.4%, respectively. In major veins, however, significantly more HDM was produced in C123; 12.3% of the small metaxylem vessels were occluded in B14A as opposed to 26.4% in C123. No large metaxylem vessels were occluded in B14A, whereas 30% were occluded in C123.

Intercellular material, thought to be of host origin, was seen in the mesophyll tissue of some infected leaves (Fig. 21). Although this material occurred in B14A, it was observed more commonly in C123. This material was Schiff-positive and could be differentiated from EPS because it stained deep blue as opposed to reddish-purple with toluidine blue O.

Widespread cell wall disruption occurred only during the late stages of pathogenesis (Fig. 23). Secondary thickenings in xylem cell walls separated from the rest of the cell wall as degradation progressed. Necrosis of vascular parenchyma and bundle sheath cells occurred only after pathogen populations in vessels had become high. Generally, starch was lost from chloroplasts of bundle sheath cells, and the plastids became randomly arranged preceding death of bundle sheath cells. Extensive membrane damage and collapse of mesophyll cells occurred during the last stages of pathogenesis (Fig. 24). Bacterial cells often could be seen among collapsed mesophyll cells within the lesion margins and abundant EPS was produced in this tissue.

DISCUSSION

Resistance to the leaf blight phase of the Stewart's wilt disease is characterized by a reduced rate of lesion expansion in the resistant host. This type of resistance could result from a reduced rate of pathogen growth in the resistant host and (or) a host response that serves to localize the infection. The growth rate of *E. stewartii* was similar in B14A and C123 seedlings. These findings are in agreement with those of others who studied population dynamics of *E. stewartii* in resistant and susceptible maize seedlings (23). Observations presented here suggest that resistance is not due to reduced pathogen growth rates. This conclusion should be viewed with some caution, however, since growth in seedling leaves may not be analogous to growth in mature leaf tissue. Although it would have been desirable to examine population dynamics in leaves of mature maize plants, technical difficulties made uniform inoculation of such plants impossible.

Accumulation of host-derived materials (HDM) in vessels of plants infected with phytopathogenic bacteria seems to be a common phenomenon (12,13,20,21). It has been suggested that these materials might function in disease resistance or may be the product of a resistance reaction (12,20). At least four different kinds of HDM were found in vessels of infected maize plants. In addition to physically impeding the movement of bacteria in the xylem, some of the materials possibly had antibacterial properties. In either instance, that these vessel-plugging materials were formed more frequently in C123 than B14A suggests that they might function in the localization of the pathogen. Tyloses, which are thought to restrict the spread of some wilt-inducing bacteria (12), were not observed in the infected maize plants.

Bacterial EPS have long been thought to play an important role in the development of bacterial wilts, and EPS (or slime) production has been correlated with aggressiveness in several wilt-inducing bacteria (1,10,15,17,18). High-molecular-weight EPSs are thought to interfere with water movement by mechanically plugging vessels (9,10,17) and by increasing the viscosity of water within them (10). High-molecular-weight polysaccharides are thought to disrupt vascular flow at very low concentrations by accumulation on pit membranes (19). Although the material observed coating pit membranes was not positively identified, it was assumed to be bacterial EPS. This material was found on pit membranes during the very early stages of pathogenesis. In many

Figs. 19–24. Reactions of resistant and susceptible maize inbred lines infected with *Erwinia stewartii*. **19,** Host-derived material (HDM), bacterial cells (B), and exopolysaccharide (EPS) in a narrow metaxylem vessel of a major vein in B14A. HDM stained light blue with toluidine blue (TB) and was Schiff-positive and Sudan black B (SB)-negative. Sample taken at lesion margin 2 wk after inoculation. Bar represents 1 μm. **20,** HDM in wide metaxylem vessel of C123. HDM stained blue-green with TB, but the color faded within a few days. SB- and Schiff-negative. Cell wall (cw) separates vessel from moribund parenchyma cell. Collected 1 cm inside lesion margin 2 wk after inoculation. Bar represents 1 μm. **21,** Host-derived intercellular material (IM) between two mesophyll cells (ME) in C123 leaf. IM stained blue with TB, was Schiff-positive, and SB-negative. Collected 0.5 cm from inoculation wounds 1 wk after inoculation. Bar represents 1 μm. **22,** HDM in wide metaxylem vessel of C123 leaf. Staining characteristics are the same as HDM in Fig. 20. Collected 1 cm inside lesion margin 2 wk after inoculation. Bar represents 1 μm. **23,** Bacteria (B) in narrow metaxylem of major vein in B14A leaf. Cell wall (cw) has ruptured between vessel (left) and parenchyma cell (right). Secondary thickening (arrow) appears to be separating from vessel wall. Bar represents 1 μm. **24,** Light micrograph of B14A leaf with several plugged narrow metaxylem vessels in major vein to the left and minor vein to the right. Bundle sheath and mesophyll cells have collapsed. Sample taken 1 cm inside lesion margin 3 wk after inoculation. Bar represents 10 μm.

instances, pit membranes were coated in areas where few bacterial cells were seen. This suggests that EPS is effectively filtered out of the transpiration stream by pit membranes. Large accumulations of EPS seemed to have no adverse effect on nearby parenchyma or mesophyll cells, indicating that the EPS of *E. stewartii* does not act as a cellular toxin.

Wellhausen (22) observed distinct histopathological reactions in maize seedlings infected with *E. stewartii*. Vessels became plugged rapidly and the vascular bundle and surrounding tissues were rapidly destroyed in susceptible seedlings. In moderately resistant cultivars, xylem parenchyma became hyperplastic and lignified and the vessels gradually became plugged. In resistant seedlings, hyperplasia and lignification did not occur, and only slight plugging of vessels was observed. In the present study, these distinct reactions were not seen in the leaves of mature maize plants. Hyperplasia of xylem parenchyma did not occur, and significant plugging of vessels occurred in the lesion areas of resistant as well as of susceptible plants.

The extensive disruption of parenchyma and mesophyll cells seen in later stages of pathogenesis could have been due to desiccation of infected tissues. Bundle sheath cells in lesion areas contained randomly arranged plastids, which often lacked starch. These alterations also have been reported in bundle sheath cells of corn plants exposed to water stress (8). In addition, many cells in lesion areas were plasmolyzed, tonoplasts were often disrupted, and cells eventually collapsed. Similar alterations are often seen in water-stressed plant cells (7,8).

LITERATURE CITED

1. Ayers, A. R., Ayers, S. B., and Goodman, R. N. 1979. Extracellular polysaccharide of *Erwinia amylovora*: a correlation with virulence. Appl. Environ. Microbiol. 38:659-666.
2. Chang, C.-M., Hooker, A. L., and Lim, S. M. 1977. An inoculation technique for determining Stewart's bacterial leaf blight reaction in corn. Plant Dis. Rep. 61:1077-1079.
3. Dye, D. W. 1968. A taxonomic study of the genus *Erwinia*. I. The "amylovora" group. N. Z. J. Sci. 11:590-607.
4. Dye, D. W. 1969. A taxonomic study of the genus *Erwinia*. II. The "herbicola" group. N. Z. J. Sci. 12:223-226.
5. Esau, K. 1943. Ontogeny of the vascular bundle in *Zea mays*. Hilgardia 15:327-368.
6. Esau, K. 1977. Anatomy of Seed Plants. 2nd ed. John Wiley & Sons, New York. 550 pp.
7. Fellows, R. J., and Boyer, J. S. 1978. Altered ultrastructure of cells of sunflower leaves having low water potentials. Protoplasma 93:381-395.
8. Giles, K. L., Beardsell, M. F., and Cohen, D. 1974. Cellular and ultrastructural changes in mesophyll and bundle sheath cells of maize in response to water stress. Plant Physiol. 54:208-212.
9. Harris, H. A. 1940. Comparative wilt induction by *Erwinia tracheiphila* and *Phytomonas stewartii*. Phytopathology 30:625-638.
10. Husain, A., and Kelman, A. 1958. Relation of slime production to mechanism of wilting and pathogenicity of *Pseudomonas solanacearum*. Phytopathology 48:155-165.
11. Ivanoff, S. S. 1933. Stewart's wilt disease of corn, with emphasis on the life history of *Phytomonas stewartii* in relation to pathogenesis. J. Agric. Res. 47:749-770.
12. Mollenhauer, H. H., and Hopkins, D. L. 1976. Xylem morphology of Pierce's disease-infected grapevines with different levels of tolerance. Physiol. Plant Pathol. 9:95-100.
13. Nelson, P. E., and Dickey, R. S. 1970. Histopathology of plants infected with vascular bacterial pathogens. Annu. Rev. Phytopathol. 8:259-280.
14. Parham, R. A., and Kaustinen, H. M. 1976. Differential staining of tannin in sections of epoxy-embedded plant cells. Stain Technol. 51:237-240.
15. Pepper, E. H. 1967. Stewart's bacterial wilt of corn. Phytopathological Monograph 4. American Phytopathological Society. Worcester, MA. 36 pp.
16. Pool, C. R. 1973. Prestaining oxidation by acidified hydrogen peroxide for revealing Schiff-positive sites in Epon-embedded sections. Stain Technol. 48:123-126.
17. Sutton, J. C., and Williams, P. H. 1970. Relation of xylem plugging to black rot lesion development in cabbage. Can. J. Bot. 48:391-401.
18. Sutton, J. C., and Williams, P. H. 1970. Comparison of extracellular polysaccharide of *Xanthomonas compestris* from culture and from infected cabbage leaves. Can. J. Bot. 48:645-651.
19. Van Alfen, N. K., and Allard-Turner, V. 1979. Susceptibility of plants to vascular disruption by macromolecules. Plant Physiol. 63:1072-1075.
20. Wallis, F. M., Rijkenberg, F. H. J., Joubert, J. J., and Martin, M. M. 1973. Ultrastructural histopathology of cabbage leaves infected with *Xanthomonas campestris*. Physiol. Plant Pathol. 3:371-378.
21. Wallis, F. M., and Truter, S. J. 1978. Histopathology of tomato plants infected with *Pseudomonas solanacearum*, with emphasis on ultrastructure. Physiol. Plant Pathol. 13:307-317.
22. Wellhausen, E. J. 1936. Genetics of resistance to bacterial wilt in maize. Ph.D. dissertation, Iowa State College, Ames. 158 pp.
23. Wodds, T. J., and Sherf, A. F. 1979. Population dynamics of *Erwinia stewartii* in leaves of sweet and field corn hybrids tolerant and susceptible to Stewart's disease. (Abstr. 226) Proc. IX Int. Congr. Plant Prot. 5–11 August 1979. Washington DC.